

**Mapping dark matter in the gamma-ray sky with galaxy catalogs**Shin'ichiro Ando,<sup>1</sup> Aurélien Benoit-Lévy,<sup>2</sup> and Eiichiro Komatsu<sup>3,4</sup><sup>1</sup>*GRAPPA Institute, University of Amsterdam, 1098 XH Amsterdam, The Netherlands*<sup>2</sup>*Department of Physics and Astronomy, University College London, London WC1E 6BT, United Kingdom*<sup>3</sup>*Max-Planck-Institut für Astrophysik, Karl-Schwarzschild Strasse 1, 85741 Garching, Germany*<sup>4</sup>*Kavli Institute for the Physics and Mathematics of the Universe (Kavli IPMU, WPI), Todai Institutes for Advanced Study, The University of Tokyo, Kashiwa, Chiba 277-8583, Japan*

(Received 16 December 2013; revised manuscript received 25 March 2014; published 10 July 2014)

Cross correlating gamma-ray maps with locations of galaxies in the low-redshift Universe *vastly* increases sensitivity to signatures of annihilation of dark matter particles. Low-redshift galaxies are ideal targets, as the largest contribution to anisotropy in the gamma-ray sky from annihilation comes from  $z \lesssim 0.1$ , where we expect minimal contributions from astrophysical sources such as blazars. Cross correlating the five-year data of Fermi-LAT with the redshift catalog of the 2MASS survey can detect gamma rays from annihilation if dark matter has the canonical annihilation cross section and its mass is smaller than  $\sim 100$  GeV.

DOI: [10.1103/PhysRevD.90.023514](https://doi.org/10.1103/PhysRevD.90.023514)

PACS numbers: 95.35.+d, 95.80.+p, 95.85.Pw, 98.70.Vc

**I. INTRODUCTION**

If dark matter particles annihilate and produce gamma rays, as predicted for a popular class of dark matter candidates, we can detect them in *anisotropy* in the gamma-ray sky, since the sites of annihilation trace the inhomogeneous matter distribution in the Universe [1]. Gamma-ray anisotropy has been studied theoretically [1–17] and recently detected with the 22-month data of the Fermi Large Area Telescope (LAT) [18]. This signal, however, can be explained entirely by active galaxies called blazars [19]. The current upper bounds on the rate of dark matter annihilation obtained from gamma-ray anisotropy data are still too weak to test the most interesting parameter regions, in which the dark matter mass is on the order of 100 GeV and the annihilation cross section is  $\langle\sigma v\rangle = 3 \times 10^{-26} \text{ cm}^3 \text{ s}^{-1}$  [17,20], as implied from thermal production mechanisms [21].

The current bounds are weak because the Fermi-LAT data at high energies ( $\sim 10$  GeV), which are sensitive to dark matter masses of  $\sim 100$  GeV, are still totally photon-noise dominated. One way to extract signals more efficiently in such a low signal-to-noise regime is to *cross correlate* the noise-dominated data with some signal-dominated data whose signals are spatially well correlated with those in the noise-dominated data.

In this paper, we show that the *existing* catalog of locations of galaxies in the low-redshift Universe ( $z \lesssim 0.1$ ) measured by the spectroscopic follow-up observations of the Two Micron All Sky Survey (2MASS) [22] provides an excellent template, which vastly increases sensitivity to dark matter annihilation in cross correlation with the Fermi-LAT data. We find that the expected sensitivity from the five-year Fermi data is stringent enough to probe the most interesting parameter regions of the

annihilation cross section for large ranges of dark matter masses, although the exact limits are still subject to uncertainties on the abundance of dark matter substructures. We also show that the existing upper limits on the cross correlation of the 21-month Fermi data with galaxy catalogs [23] already yield much improved limits on the dark matter properties. Cross correlation of the gamma-ray data with gravitational lensing data can also be used to increase sensitivity to dark matter annihilation, as shown by Ref. [24].

**II. INTENSITY OF THE DIFFUSE GAMMA-RAY BACKGROUND**

The mean intensity of the diffuse gamma-ray background due to dark matter annihilation (the number of photons received per unit area, time, solid angle, and energy range) is given by

$$I_{\text{dm}}(E) = \int d\chi W_{\text{dm}}([1+z]E, \chi) \langle\delta^2(z)\rangle, \quad (1)$$

where  $\chi$  is the comoving distance out to a given redshift  $z$ . A window function,

$$W_{\text{dm}}(E, z) = \frac{\langle\sigma v\rangle}{8\pi} \left(\frac{\Omega_{\text{dm}}\rho_c}{m_{\text{dm}}}\right)^2 (1+z)^3 \frac{dN_{\gamma,\text{ann}}}{dE} e^{-\tau}, \quad (2)$$

contains all the particle-physics information such as the annihilation cross section  $\langle\sigma v\rangle$ , the dark matter mass  $m_{\text{dm}}$ , the energy spectrum of emitted gamma rays per annihilation,  $dN_{\gamma,\text{ann}}/dE$ , and the optical depth of absorption during propagation in the intergalactic space,  $\tau(E, z)$  (e.g., [25]). We use  $\Omega_{\text{dm}} = 0.23$  for the density parameter of dark matter, and  $\rho_c$  is the present critical density of the

Universe. The variance of the matter density fluctuation,  $\langle \delta^2 \rangle$ , is given by

$$\langle \delta^2 \rangle = \left( \frac{1}{\Omega_m \rho_c} \right)^2 \int dM \frac{dn(M, z)}{dM} [1 + b_{\text{sh}}(M)] \times \int dV \rho_{\text{host}}^2(r|M), \quad (3)$$

where  $dn/dM$  is the comoving number density of dark matter halos per unit mass range,  $\rho_{\text{host}}(r|M)$  is the density profile of dark matter halos of mass  $M$ , and  $b_{\text{sh}}(M)$  is the so-called ‘‘boost factor’’ due to the presence of subhalos inside parent dark matter halos. See Ref. [17] for how to evaluate Eq. (3) as well as for the cosmological parameters used in the calculation. The boost factor  $b_{\text{sh}}$  depends on the minimum mass of possible subhalos as well as on the host halo mass. For the minimum subhalo mass, we use the standard value for the cold dark matter particles,  $10^{-6} M_\odot$ .

Let us specify some important details of the model. As the rate of annihilation depends on local density squared, the results are sensitive to how clumpy dark matter halos are. There are two important quantities related to clumpiness. One is the so-called ‘‘concentration parameter’’ of the density profile of halos, and we use the model developed in Ref. [26] for  $M < 2.5 \times 10^{14} M_\odot$  and that in Ref. [27] otherwise. This model yields results similar to the latest work [28]. We find that most of the contributions to the anisotropy come from subhalos inside the large-mass halos ( $M \gtrsim 10^{10} M_\odot$ ) at low redshifts ( $z \lesssim 0.1$ ) [17]. The concentration parameters of such large-mass halos have been well characterized. Another important quantity is the boost factor due to subhalos, and we use the model developed by Gao *et al.* [29]. Their power-law scaling with mass,  $b_{\text{sh}} \propto M^{0.39}$ , was recently challenged by Sánchez-Conde and Prada [30], who claim to find significantly weaker dependence of  $b_{\text{sh}}$  on  $M$ . This greatly reduces the amplitude of anisotropies as well as the mean intensity. While we continue to adopt the model of Ref. [29] as the main model in this paper, our conclusion changes if the model of Ref. [30] turns out to be correct. This is the largest uncertainty in our model, and it is common to *all* the extragalactic constraints discussed in the literature.

In Fig. 1, we show  $I_{\text{dm}}(E)$  from annihilation of 100-GeV dark matter purely into  $b\bar{b}$  with  $\langle \sigma v \rangle = 3 \times 10^{-26} \text{ cm}^3 \text{ s}^{-1}$ , as well as from two astrophysical sources: blazars and star-forming galaxies. For both populations, we treat spectrally hard and soft subpopulations separately: BL Lacs ( $E^{-2.1}$ ) and flat-spectrum radio quasars ( $E^{-2.4}$ ) for the blazars; starbursts ( $E^{-2.2}$ ) and normal spirals ( $E^{-2.7}$ ) for the star-forming galaxies. The mean intensity of these sources is computed in a similar manner to dark matter, using Eq. (1) but by replacing  $W_{\text{dm}}$  with a window function of each population and  $\langle \delta^2 \rangle$  with 1 (as they trace density). The window function  $W_X$ , where  $X$  represents either star-forming galaxies or blazars, is given by

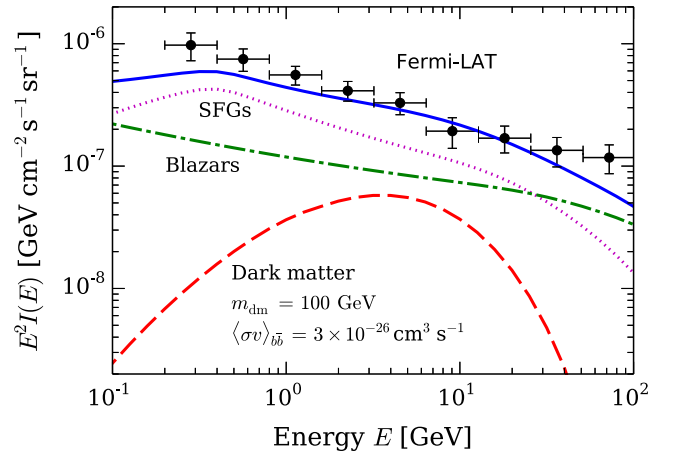


FIG. 1 (color online). Predicted mean intensity spectra of diffuse gamma-ray background. The dashed, dot-dashed, and dotted lines show the contributions from dark matter annihilation (parameters adopted are also shown), blazars, and star-forming galaxies (labeled as SFGs), respectively. The solid line shows the sum, while the points with error bars show the Fermi-LAT data [35].

$$W_X([1+z]E, z) = \chi^2 \int_0^{\mathcal{L}_{\text{lim}}} d\mathcal{L} \Phi_X(\mathcal{L}, z) \mathcal{F}_X(\mathcal{L}, z), \quad (4)$$

where  $\mathcal{L}$  is the differential luminosity (i.e., the number of gamma-ray photons emitted per unit time, per unit energy range) at energy  $(1+z)E$ , and  $\mathcal{F}_X(\mathcal{L}, z) = (1+z)^2 \mathcal{L} / (4\pi d_L^2)$  is the differential number flux at energy  $E$  from a source  $X$  at  $z$ . The upper limit of the integration  $\mathcal{L}_{\text{lim}}$  corresponds to the flux sensitivity of Fermi,  $F_{\text{lim}}$ , integrated above 100 MeV, and we adopt  $F_{\text{lim}} = 4 \times 10^{-9} \text{ cm}^{-2} \text{ s}^{-1}$  ( $3 \times 10^{-8} \text{ cm}^{-2} \text{ s}^{-1}$ ) for hard (soft) sources. For the luminosity function  $\Phi_X$  for blazars, we adopt the luminosity-dependent density evolution model separately for BL Lacs [31] and flat-spectrum radio quasars [32], which both roughly behave as a broken power law in luminosity. For the luminosity function of star-forming galaxies, we adopt the infrared luminosity function [33], which behaves as a power law with a cutoff luminosity, again separately for spiral and starburst galaxies. Finally, such an infrared luminosity function is converted to the gamma-ray luminosity function by using the correlation between infrared and gamma-ray luminosity calibrated with Fermi:  $L_\gamma \propto L_{\text{IR}}^{1.17}$  [34].

Figure 1 shows that the annihilation signal is below the current measurements as well as the predicted astrophysical contributions. This situation, however, changes completely when we consider the cross correlation of anisotropies.

### III. CROSS CORRELATION WITH 2MASS GALAXY CATALOG

We consider the cross-correlation power spectrum  $C_\ell^{\text{dm.g}}$  between the fluctuations in the gamma-ray intensity  $\delta I_{\text{dm}}$  and the galaxy density contrast  $\delta_g$ . It is defined by

$$\langle \delta I_{\text{dm}}(\hat{\mathbf{n}}) \delta_{\text{g}}(\hat{\mathbf{n}} + \boldsymbol{\theta}) \rangle = \sum_{\ell} \frac{2\ell + 1}{4\pi} C_{\ell}^{\text{dm,g}} P_{\ell}(\cos \theta), \quad (5)$$

where  $P_{\ell}(\cos \theta)$  is the Legendre polynomial. Each multipole roughly corresponds to an angular size of  $\theta \approx \pi/\ell$ . We compute  $C_{\ell}^{\text{dm,g}}$  as

$$C_{\ell}^{\text{dm,g}} = \int \frac{d\chi}{\chi^2} W_{\text{dm}}(\chi) W_{\text{g}}(\chi) P_{\delta^2, \text{g}} \left( k = \frac{\ell}{\chi}, \chi \right), \quad (6)$$

where  $W_{\text{g}}$  is the galaxy window function, normalized to unity after integration over  $\chi$ . The angular cross-power spectrum is determined by the three-dimensional cross-power spectrum of  $\delta^2$  and galaxies,  $P_{\delta^2, \text{g}}(k)$ . We model this power spectrum as  $P_{\delta^2, \text{g}}(k) = b_{\text{g}} P_{\delta^2, \delta}(k)$ , where  $b_{\text{g}}$  is the so-called galaxy bias factor. We use  $b_{\text{g}} = 1.4$  for galaxies in the 2MASS catalog [36].

To compute  $P_{\delta^2, \delta}(k)$ , we extend the formalism given in Ref. [17] to the cross correlation and obtain  $P_{\delta^2, \delta} = P_{\delta^2, \delta}^{1h} + P_{\delta^2, \delta}^{2h}$ , where

$$P_{\delta^2, \delta}^{1h} = \left( \frac{1}{\Omega_m \rho_c} \right)^3 \int dM \frac{dn}{dM} \tilde{u}(k|M) \tilde{v}(k|M) M \times [1 + b_{\text{sh}}(M)] \int dV \rho_{\text{host}}^2(r|M), \quad (7)$$

$$P_{\delta^2, \delta}^{2h} = \left( \frac{1}{\Omega_m \rho_c} \right)^2 \left\{ \int dM \frac{dn}{dM} \tilde{u}(k|M) b_1(M, z) \times [1 + b_{\text{sh}}(M)] \int dV \rho_{\text{host}}^2(r|M) \right\} \times \left[ \int dM \frac{dn}{dM} M \tilde{v}(k|M) b_1(M, z) \right] P_{\text{lin}}(k, z), \quad (8)$$

where  $P_{\text{lin}}(k, z)$  is the linear matter power spectrum,  $b_1(M, z)$  is the linear halo bias, and  $\tilde{u}(k|M)$  and  $\tilde{v}(k|M)$  are the Fourier transform of gamma-ray emissivity and density profiles, respectively, which are both normalized to unity after integration over volume.

For the cross correlation of the astrophysical sources with 2MASS galaxies, we use Eq. (6) with a proper replacement of  $W_{\text{dm}}$  with the astrophysical window function [Eq. (4)]. We also replace the power spectrum  $P_{\delta^2, \text{g}}$  with  $P_{X, \text{g}}$ , and we approximate it as  $P_{X, \text{g}} \approx b_X b_{\text{g}} P_{\delta}$ , where  $P_{\delta}$  is the matter power spectrum. For both blazars and star-forming galaxies, we assume  $b_X = 1.4$  for their bias parameters.

The angular power spectrum defined by Eq. (6) has units of intensity times solid angle, and it is proportional to  $\langle \sigma v \rangle$ . In Fig. 2, we show the predicted  $C_{\ell}^{\text{dm,g}}$  with the 2MASS Redshift Survey [22], assuming  $\langle \sigma v \rangle = 3 \times 10^{-26} \text{ cm}^3 \text{ s}^{-1}$  in the energy range of 5–10 GeV, for 100-GeV dark matter annihilating into  $b\bar{b}$ . We also show the predicted cross spectra with the 2MASS Redshift Survey for blazars and

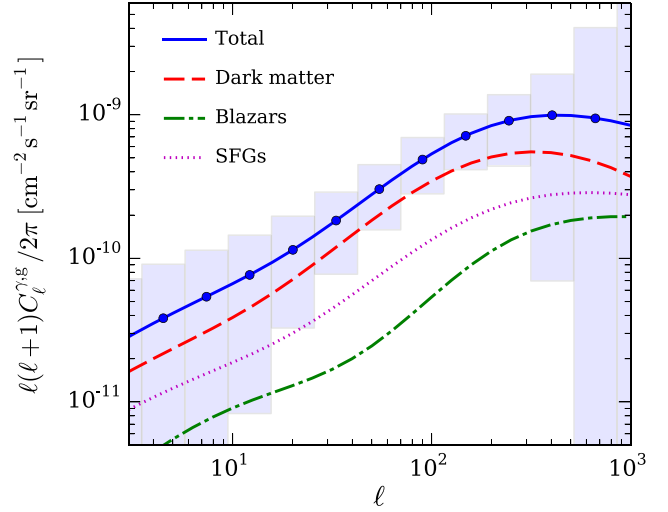


FIG. 2 (color online). Predicted angular cross-power spectra of gamma-ray emission in 5–10 GeV and the distribution of galaxies measured by the 2MASS Redshift Survey. The dashed, dot-dashed, and dotted lines show the contributions from dark matter annihilation, blazars, and star-forming galaxies, respectively. The solid line shows the sum, while the points with the boxes show the errors expected after five-year observations of Fermi-LAT. The particle physics model is the same as in Fig. 1.

star-forming galaxies, respectively. Remarkably, we find that the dark matter–galaxy correlation dominates over the other astrophysical contributions. This is because the low-redshift ( $z \lesssim 0.1$ ) 2MASS galaxies are less correlated with the astrophysical gamma-ray sources than with dark matter annihilation. The galactic emission due to cosmic ray interactions is much more concentrated at the halo center than dark matter annihilation; thus, while the former is easier to identify with nearby individual sources, the latter yields the larger luminosity density in a local volume.<sup>1</sup> It is therefore important to use a local galaxy catalog such as 2MASS to reduce contamination from blazars and star-forming galaxies.

In Fig. 3, we show the cross-correlation coefficients  $C_{\ell}^{\gamma, \text{g}} / \sqrt{C_{\ell}^{\gamma} C_{\ell}^{\text{g}}}$  between gamma rays from dark matter, blazars, or star-forming galaxies, and the 2MASS galaxies. We find that the gamma rays from dark matter annihilation and the 2MASS galaxies are spatially well correlated, with cross-correlation coefficients of about 0.8 over a wide range of multipoles up to  $\ell \approx 200$ . On the other hand, blazars are poorly correlated, having negligible cross-correlation coefficients. This is because, as far as we know, there are not

<sup>1</sup>For example, several star-forming galaxies in the local volume such as M31 were detected with Fermi, and they are all consistent with cosmic-ray origin [34]. This, however, does not exclude the possibility that the entire local volume contains more gamma rays due to dark matter annihilation than to cosmic rays. This is because, even if a galaxy identified with Fermi emits the same amount of photons from dark matter annihilation, they give much smaller surface brightness, and hence would not be detected, as dark matter is distributed out to a virial radius.

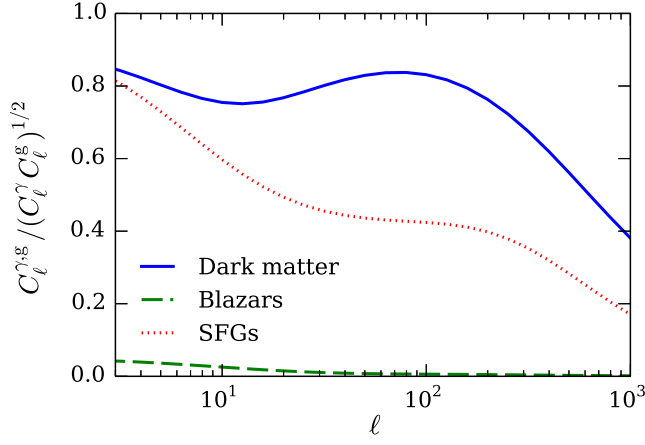


FIG. 3 (color online). Predicted cross-correlation coefficients  $C_\ell^{\gamma g} / \sqrt{C_\ell^\gamma C_\ell^g}$  between gamma rays from dark matter (solid line), blazars (dashed line), or star-forming galaxies (dotted line), and the 2MASS Redshift Survey galaxies.

many blazars in the local Universe (with the assumed lowest gamma-ray luminosity of  $10^{42}$  erg s $^{-1}$  above 100 MeV). Star-forming galaxies are also less correlated, having the cross-correlation coefficients of  $\lesssim 0.5$  at  $\ell \gtrsim 10$ .

Another remarkable finding from Fig. 2 is that the existing data, i.e., the five-year data of Fermi-LAT and the galaxies in the 2MASS Redshift Survey, have sufficient sensitivity to detect gamma rays from dark matter annihilation with the canonical annihilation cross section and  $m_{\text{dm}} = 100$  GeV. To compute the predicted error bars, we use

$$\delta C_\ell^{\gamma g} = \sqrt{\frac{1}{(2\ell+1)f_{\text{sky}}}} \left[ (C_\ell^{\gamma g})^2 + \left( C_\ell^\gamma + \frac{C_N^\gamma}{W_\ell^2} \right) (C_\ell^g + C_N^g) \right]^{1/2}, \quad (9)$$

where  $f_{\text{sky}} = 0.7$  is a fraction of the sky used for the analysis. For the autocorrelation power spectrum  $C_\ell^\gamma$ , we use the measured values reported in Ref. [18], and the photon noise is estimated as  $C_N^\gamma = I_{\text{obs}}/\mathcal{E}$ , where  $I_{\text{obs}}$  is the observed mean intensity reported in Ref. [35] and  $\mathcal{E} = 1.5 \times 10^{11}$  cm $^2$  s is the exposure for the five-year Fermi-LAT operation (almost independent of energy). As for the window function of the Fermi-LAT angular response,  $W_\ell$ , we use a functional form that approximates the results reported in Ref. [18]. It is straightforward to calculate the angular power spectrum of the galaxies,  $C_\ell^g$ , from the redshift distribution of galaxies in the 2MASS Redshift Survey (see, e.g., [12]). Finally,  $C_N^g$  is the shot noise of galaxies given by  $C_N^g = 4\pi f_{2\text{MASS}}/N_g$ , where  $N_g = 43500$  is the number of 2MASS galaxies with measured redshifts over  $f_{2\text{MASS}} = 0.91$  of the sky.

A simple error propagation gives the expected uncertainties on theoretical parameters,  $\{\vartheta_a\}$ , given the errors on the power spectrum. We first compute the Fisher matrix

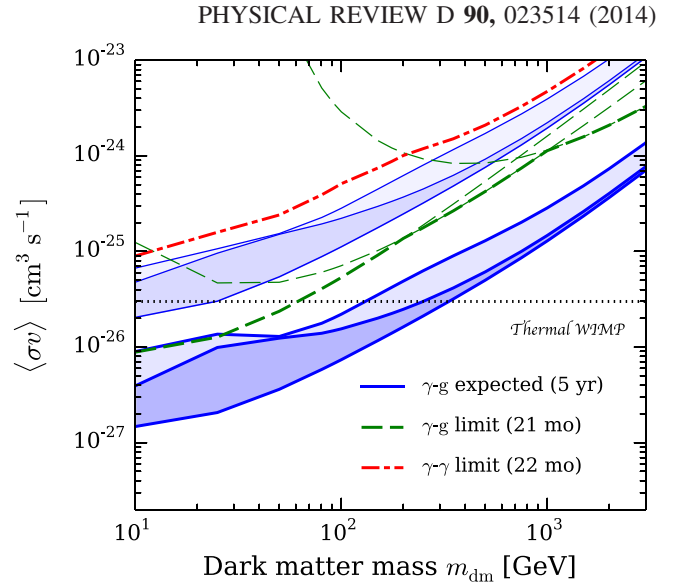


FIG. 4 (color online). Existing and expected 95% CL upper bounds on the cross section of annihilation into  $b\bar{b}$ . The dot-dashed line shows the bounds from the auto-power spectrum of the 22-month Fermi-LAT data [17], while the dashed lines show the bounds from the cross-power spectra between the 21-month Fermi-LAT data ( $E > 1, 3,$  and  $30$  GeV from the left to right) and the 2MASS galaxies (with photometric redshifts) that we derive using the measurement reported in Ref. [23]. The solid curves show the expected bounds from the five-year Fermi-LAT data cross correlated with galaxies in the 2MASS Redshift Survey, based on the assumption that all the astrophysical contributions (lower), only blazars (middle), or none of them (upper) are understood. The lower, thick solid curves are derived using the boost factor model of Ref. [29], whereas the upper, thin solid curves are based on Ref. [30].

$$F_{ab} = \sum_\ell \sum_i \frac{(\partial C_{\ell,i}^{\gamma g} / \partial \vartheta_a)(\partial C_{\ell,i}^{\gamma g} / \partial \vartheta_b)}{(\delta C_{\ell,i}^{\gamma g})^2}, \quad (10)$$

where  $\vartheta_1 = \langle \sigma v \rangle$  and  $\vartheta_2$  and  $\vartheta_3$  are the amplitudes of the cross spectra for the star-forming galaxies and blazars, respectively, the subscript  $i$  represents four energy bands (1–2, 2–5, 5–10, and 10–50 GeV), and  $\delta C_{\ell,i}^{\gamma g}$  in the denominator is evaluated using Eq. (9) at  $\langle \sigma v \rangle = 3 \times 10^{-26}$  cm $^3$  s $^{-1}$ .<sup>2</sup> The covariance between different energy ranges is negligible, as the auto-power spectrum of the gamma-ray data is dominated by shot noise of the photons. The 95% CL upper bound on  $\langle \sigma v \rangle$  is then obtained with  $\langle \sigma v \rangle < 1.64 \sqrt{(F^{-1})_{11}}$ .

The lowest thick solid curve in Fig. 4 shows the most optimistic constraint obtained by assuming that we know the amplitudes of contributions from star-forming galaxies and blazars, i.e.,  $\langle \sigma v \rangle < 1.64 / \sqrt{F_{11}}$ . The second to lowest

<sup>2</sup>While the error  $\delta C_{\ell,i}^{\gamma g}$  also depends on  $\langle \sigma v \rangle$ , the dependence is weak because it is dominated by the photon shot noise. We thus fix  $\langle \sigma v \rangle$  to be the canonical value in  $\delta C_{\ell,i}^{\gamma g}$  when computing the Fisher matrix.

curve shows the realistic bound obtained by varying the amplitudes of contributions from dark matter and star-forming galaxies (i.e., the Fisher matrix is a  $2 \times 2$  matrix for  $\vartheta_1$  and  $\vartheta_2$ ). Finally, the upper thick solid curve shows the conservative bound obtained by varying all  $\vartheta_a$ 's; i.e., this bound is obtained by using no prior knowledge on the amplitudes. This is conservative because we know that the blazar contribution is tightly constrained to be negligible from its luminosity function [31,32] and the angular power spectrum [19], and thus the error associated with this component is much smaller.

The existing bounds on  $\langle\sigma v\rangle$  from the auto-power spectra of the 22-month Fermi-LAT [17] data are shown by the dot-dashed line. The five-year cross spectra can improve the constraints by more than 1 order of magnitude, testing the most interesting parameter space of the dark matter masses and cross sections.

One partial reason for the improvement over the auto-power spectrum is that the analysis of the auto-power spectrum is limited to  $\ell \geq 155$  due to potential contamination by the diffuse Galactic emission [18], whereas we can use the entire multipoles for the cross-power spectrum, as the Galactic emission is not correlated with the locations of 2MASS galaxies.

This conclusion is subject to the theoretical uncertainty regarding the boost factor  $b_{\text{sh}}(M)$ . The model of Ref. [29] relies on an extrapolation of a power-law relation between the concentration parameter and the halo mass. Reference [30] argues that such a power-law extrapolation to very small masses is unphysical, and the relation must necessarily flatten toward lower masses, resulting in substantially fainter subhalos in parent halos with  $M \gtrsim 10^{10} M_\odot$ . If we adopt the latter model [30], the amplitude of the cross correlation shown in Fig. 2 is reduced, while there is little change in its shape. The thin solid curves in Fig. 4 show the expected five-year constraints using the same model. In this case the constraints weaken by an order of magnitude. This represents the current theoretical uncertainty in the prediction.

#### IV. 21-MONTH UPPER LIMITS FROM CROSS-CORRELATION STUDY

What do the current data tell us? Xia *et al.* [23] have measured the cross-correlation function in configuration space,  $C(\theta)$ , from the 21-month Fermi-LAT data and 770000 2MASS galaxies with photometric (rather than spectroscopic) redshifts over the angular range of 1–10 degrees. They found no evidence for cross correlation. Thus, we use our model to place upper bounds on  $\langle\sigma v\rangle$  from their measurements, by fixing components of the star-forming galaxies and blazars to their baseline models. We compute the  $\chi^2$  statistics:

$$\chi^2 = \sum_{ij} [C^{\gamma,g}(\theta_i) - C_i] (\delta C^2)_{ij}^{-1} [C^{\gamma,g}(\theta_j) - C_j], \quad (11)$$

where  $C^{\gamma,g}(\theta)$  is the theoretical value of the cross-correlation function corresponding to  $C_\ell^{\gamma,g}$ ,  $C_i$  is the measured cross correlation in the  $i$ th angular bin, and  $(\delta C^2)_{ij}^{-1}$  is the inverse covariance matrix computed from the jackknife analysis [23]. The dashed lines in Fig. 4 show the 95% CL upper bounds on  $\langle\sigma v\rangle$  from the measurements in  $E > 1, 3,$  and 30 GeV. The existing data indeed provide a significant improvement over the auto-power spectrum. This analysis thus provides a proof of concept.

## V. DISCUSSION AND CONCLUSIONS

### A. Other possible astrophysical sources

There are other astrophysical source classes that trace dark matter and contribute to the gamma-ray background. Misaligned active galaxies are one such example, and it has been shown that they could give a larger contribution to the mean intensity than blazars, although with much larger uncertainties (see, e.g., Ref. [37]). Our Fisher-matrix approach adopted in Sec. III, however, relies on no prior information on the amplitudes of the cross-power spectrum for both the blazars and star-forming galaxies, with which we still obtain quite stringent upper limits on the dark matter annihilation cross section. This is because the energy dependence on the cross-power spectrum is properly taken into account, where a characteristic spectrum of the dark matter component (Fig. 1) plays an essential role. Therefore, unless they feature an energy spectrum that is very different from a power law, contributions from any other astrophysical sources will be degenerate with either blazars or star-forming galaxies, and our conclusions will be unchanged.

### B. Uncertainty on galaxy bias

The bias parameter of the galaxy distribution is well constrained in the linear regime but to a lesser extent in the nonlinear regime. To this end, the approximation we adopted,  $\delta_g = b_g \delta$  with a constant linear bias  $b_g$ , is appropriate for the two-halo term, which dominates up to  $\ell \sim 50$ . The one-halo term dominates at higher multipoles, where the galaxy bias is likely nonlinear. The nonlinear bias tends to increase the small-scale power spectrum, which is currently difficult to predict due to uncertainties in the physics of galaxy formation. We thus assume the linear bias on small scales, but our prediction for the small-scale power may be an underestimate by a few tens of percent. However, this uncertainty on the bias for 2MASS galaxies unlikely affects the conclusions because it is common for all the gamma-ray sources, and we obtain significant statistics already from the linear regime alone.

### C. Correlation with gravitational lensing

Instead of using galaxy positions, the cross-correlation analysis can be performed with a map of projected

mass-density fields constructed from measurements of the gravitational lensing effect toward many background galaxies [24]. Such an analysis should also be pursued in order to further increase sensitivity as well as to improve robustness of the results against systematic errors.

#### D. Summary

We showed that taking cross correlations between the gamma-ray background and the 2MASS galaxy catalog provides a very strong probe of dark matter annihilation. If the mass of the dark matter particles is on the order of 100 GeV, an upper limit on the annihilation cross section that one can obtain by using five-year Fermi data will exclude its canonical value inferred from the thermal

freeze-out scenario even after taking uncertainties on astrophysical sources into account. We note, however, that this depends on the amount of substructures present in host dark matter halos.

#### ACKNOWLEDGMENTS

We acknowledge the GRAPPA workshop on “Anisotropic Universe” for providing the opportunity to initiate this study. We would like to thank J.-Q. Xia and A. Cuoco for providing us with the measurements of the cross-correlation function and its covariance matrix. This work was supported by NWO through the Vidi Grant (S. A.) and the Leverhulme Trust and STFC (A. B.-L.).

- 
- [1] S. Ando and E. Komatsu, *Phys. Rev. D* **73**, 023521 (2006).
  - [2] S. Ando, E. Komatsu, T. Narumoto, and T. Totani, *Phys. Rev. D* **75**, 063519 (2007).
  - [3] F. Miniati, S. M. Koushiappas, and T. Di Matteo, *Astrophys. J.* **667**, L1 (2007).
  - [4] A. Cuoco, J. Brandbyge, S. Hannestad, T. Haugboelle, and G. Miele, *Phys. Rev. D* **77**, 123518 (2008).
  - [5] J. M. Siegal-Gaskins, *J. Cosmol. Astropart. Phys.* **10** (2008) 040.
  - [6] S. K. Lee, S. Ando, and M. Kamionkowski, *J. Cosmol. Astropart. Phys.* **07** (2009) 007.
  - [7] M. Taoso, S. Ando, G. Bertone, and S. Profumo, *Phys. Rev. D* **79**, 043521 (2009).
  - [8] M. Fornasa, L. Pieri, G. Bertone, and E. Branchini, *Phys. Rev. D* **80**, 023518 (2009).
  - [9] J. M. Siegal-Gaskins and V. Pavlidou, *Phys. Rev. Lett.* **102**, 241301 (2009).
  - [10] S. Ando, *Phys. Rev. D* **80**, 023520 (2009).
  - [11] J. Zavala, V. Springel, and M. Boylan-Kolchin, *Mon. Not. R. Astron. Soc.* **405**, 593 (2010).
  - [12] S. Ando and V. Pavlidou, *Mon. Not. R. Astron. Soc.* **400**, 2122 (2009).
  - [13] A. Ibarra, D. Tran, and C. Weniger, *Phys. Rev. D* **81**, 023529 (2010).
  - [14] J. M. Siegal-Gaskins, R. Reesman, V. Pavlidou, S. Profumo, and T. P. Walker, *Mon. Not. R. Astron. Soc.* **415**, 1074 (2011).
  - [15] A. Cuoco, A. Sellerholm, J. Conrad, and S. Hannestad, *Mon. Not. R. Astron. Soc.* **414**, 2040 (2011).
  - [16] M. Fornasa, J. Zavala, M. A. Sanchez-Conde, J. M. Siegal-Gaskins, T. Delahaye, F. Prada, M. Vogelsberger, F. Zandanel, and C. S. Frenk, *Mon. Not. R. Astron. Soc.* **429**, 1529 (2013).
  - [17] S. Ando and E. Komatsu, *Phys. Rev. D* **87**, 123539 (2013).
  - [18] M. Ackermann *et al.* (Fermi LAT Collaboration), *Phys. Rev. D* **85**, 083007 (2012).
  - [19] A. Cuoco, E. Komatsu, and J. M. Siegal-Gaskins, *Phys. Rev. D* **86**, 063004 (2012).
  - [20] G. A. Gomez-Vargas *et al.* (Fermi-LAT Collaboration), [arXiv:1303.2154](https://arxiv.org/abs/1303.2154).
  - [21] G. Steigman, B. Dasgupta, and J. F. Beacom, *Phys. Rev. D* **86**, 023506 (2012).
  - [22] J. P. Huchra *et al.*, *Astrophys. J. Suppl. Ser.* **199**, 26 (2012).
  - [23] J.-Q. Xia, A. Cuoco, E. Branchini, M. Fornasa, and M. Viel, *Mon. Not. R. Astron. Soc.* **416**, 2247 (2011).
  - [24] S. Camera, M. Fornasa, N. Fornengo, and M. Regis, *Astrophys. J.* **771**, L5 (2013).
  - [25] R. C. Gilmore, R. S. Somerville, J. R. Primack, and A. Dominguez, *Mon. Not. R. Astron. Soc.* **422**, 3189 (2012).
  - [26] J. S. Bullock, T. S. Kolatt, Y. Sigad, R. S. Somerville, A. V. Kravtsov, A. A. Klypin, J. R. Primack, and A. Dekel, *Mon. Not. R. Astron. Soc.* **321**, 559 (2001).
  - [27] A. R. Duffy, J. Schaye, S. T. Kay, and C. Dalla Vecchia, *Mon. Not. R. Astron. Soc.* **390**, L64 (2008); **415**, L85(E) (2011).
  - [28] A. D. Ludlow, J. F. Navarro, R. E. Angulo, M. Boylan-Kolchin, V. Springel, C. Frenk, and S. D. M. White, *Mon. Not. R. Astron. Soc.* **441**, 378 (2014).
  - [29] L. Gao, C. S. Frenk, A. Jenkins, V. Springel, and S. D. M. White, *Mon. Not. R. Astron. Soc.* **419**, 1721 (2012).
  - [30] M. A. Sánchez-Conde and F. Prada, *Mon. Not. R. Astron. Soc.* **442**, 2271 (2014).
  - [31] M. Ajello *et al.*, *Astrophys. J.* **780**, 73 (2014).
  - [32] M. Ajello *et al.*, *Astrophys. J.* **751**, 108 (2012).
  - [33] C. Gruppioni *et al.*, *Mon. Not. R. Astron. Soc.* **432**, 23 (2013).
  - [34] M. Ackermann *et al.* (Fermi LAT Collaboration), *Astrophys. J.* **755**, 164 (2012).
  - [35] A. A. Abdo *et al.* (Fermi-LAT Collaboration), *Phys. Rev. Lett.* **104**, 101101 (2010).
  - [36] M. Davis, A. Nusser, K. Masters, C. Springob, J. P. Huchra, and G. Lemson, *Mon. Not. R. Astron. Soc.* **413**, 2906 (2011).
  - [37] M. Di Mauro, F. Calore, F. Donato, M. Ajello, and L. Latronico, *Astrophys. J.* **780**, 161 (2014).